Anuário do Instituto de Geociências
Universidade Federal do Rio de Janeiro
https://revistas.ufrj.br/index.php/aigeo/

ISSN 0101-9759
e-ISSN 1982-3908

Perspectives for Improvements on Real-Time GNSS Positioning with the Use of New Observables

Perspectivas para Melhorias no Posicionamento GNSS em Tempo Real com o Emprego das Novas Observáveis

Osvaldo Tavares de Camargo Junior, Paulo Sergio Oliveira Júnior, Lucas dos Santos Bezerra

Universidade Federal do Paraná, Departamento de Geomática, Curitiba, PR, Brasil
E-mails: osvaldo.tavares@ufpr.br; paulo.junior@ufpr.br; lucas.bezerra@ufpr.br
Corresponding author: Osvaldo Tavares de Camargo Junior; osvaldo.tavares@ufpr.br

Abstract

The research aims to analyze Global Navigation Satellite System (GNSS) positioning solutions using the Precise Point Positioning (PPP) method in kinematic mode, in which the position is obtained epoch by epoch through data from only one GNSS receiver, precise ephemerides, and satellite clock corrections, both with high accuracy. In this context, the adopted methodology employs the open-source software RTKLIB, which, through its data post-processing capability, enables the evaluation of kinematic PPP performance by incorporating new observables such as L5 and E5a bands, crucial for enhancing positional accuracy and mitigating multipath effects. Additionally, for survey simulations, data from the UFPR and POVE stations of the Brazilian Network for Continuous Monitoring of GNSS (RBMC) were utilized. The selected stations are located in the Northern and Southern regions of Brazil. The GNSS data were processed with the same tracking duration for a 45-minute cold-start, aimed at observing solution convergence. Subsequently, the estimated outputs in RTKLIB were obtained based on station origins using coordinates provided by SIRGAS-CON. Moreover, by utilizing precise ephemerides data, it was possible to conclude that the addition of new observables for triple-frequency positioning led to an improvement in the accuracy of the obtained coordinates, particularly in the Vertical component. In this regard, the increase in accuracy in experiments using only triple-frequency data with a 15° elevation mask was approximately 25% at the UFPR station and about ~37% at the POVE station. Furthermore, it was observed that reducing the elevation mask from 15° to 10° had a positive impact on dual-frequency positioning at the UFPR station, resulting in gains of over 3% in the East component and around ~21% in the North component compared to values obtained with the 15° mask. Similarly, during triple-frequency positioning at the POVE station, gains exceedingly approximately 16% in the North component and around ~22% in the Vertical component were observed.

Keywords: Coordinate accuracy; Elevation mask; Triple-frequency

Resumo

A pesquisa tem como objetivo analisar soluções de posicionamento pelo *Global Navigation Satellite System* (GNSS) utilizando o método *Precise Point Positioning* (PPP), em modo cinemático, no qual a posição é obtida época por época por meio de dados de apenas um receptor GNSS, efemérides precisas e correções de relógio de satélite, ambos com alta precisão. Dessa forma, a metodologia adotada emprega o software de código aberto RTKLIB, que, por meio de sua capacidade de pós-processamento de dados, permite avaliar o desempenho cinemático do PPP aplicando novas observáveis, como as bandas L5 e E5a, essenciais para melhorar a precisão posicional e mitigar os efeitos de multicaminho. Além disso, para as simulações de levantamento, utilizaram-se dados das estações UFPR e POVE da Rede Brasileira de Monitoramento Contínuo (RBMC). As estações selecionadas estão nas regiões Norte e Sul do Brasil. Os dados do GNSS foram processados com a mesma duração de rastreamento para um cold-start de 45 minutos, a fim de observar a convergência da solução. Em seguida, as saídas estimadas no RTKLIB foram obtidas com base nas origens das estações usando as coordenadas fornecidas pelo SIRGAS-CON. Adicionalmente, ao utilizar dados de efemérides precisas, foi possível concluir que a adição de novas observáveis para o posicionamento de tripla frequência resultou em uma melhoria na precisão das coordenadas obtidas, principalmente na componente Vertical. Nesse sentido, o aumento na precisão nos experimentos usando apenas tripla frequência com uma máscara de elevação de 15° foi de aproximadamente 25% na estação UFPR e cerca de ~37% na estação POVE. Além disso, observou-se que a redução da máscara de elevação de 15° para 10° teve um impacto positivo no posicionamento de dupla frequência na estação UFPR. Houve ganhos de mais de 3% na precisão da componente Leste e cerca de ~21% na componente Norte em comparação com os valores obtidos com a máscara de 15°. De maneira similar, na estação POVE, durante o posicionamento de tripla frequência, foram observados ganhos que superaram aproximadamente 16% na componente Norte e cerca de ~22% na componente Vertical.

Palavras-chave: Acurácia de coordenadas; Máscara de elevação; Tripla frequência

Received: 15 October 2023; Accepted: 22 April 2024

1 Introduction

Precise Point Positioning (PPP) (Zumberge et al. 1997) has been extensively researched, leading to the development of various online services capable of achieving sub-centimeter point positioning not only in static post-processing mode but also in real-time applications using a single Global Navigation Satellite System (GNSS) receiver (Grinter & Roberts 2013). Therefore, PPP has proven to be an excellent tool for geodetic and geodynamic applications, such as geodetic control, local and global deformation monitoring, dynamics of lithospheric plate motion, cadastral surveys, and photogrammetry (Alves, Monico & Romão 2011).

Several related works have been carried out, such as the studies of Rizos et al. (2012), Janssen and McElroy (2013), and Zanetti (2018), which evaluated whether PPP is a viable alternative for precise positioning under certain conditions and configurations. These studies promote comparative analysis between PPP and more traditional positioning techniques, such as static relative positioning. Therefore, future works related to PPP should focus on answering questions such as whether PPP is more accurate than traditional techniques, and if so, under what conditions and configurations.

Huber et al. (2010) and Grinter and Roberts (2011) provide a second contextualization, analyzing the potential and limitations of PPP. These authors discuss PPP advances in the last two decades, highlighting its current capabilities and limitations and presenting the possible direction of this technology. They conclude that PPP research advances will likely provide an increasingly wide variety of products, especially in terms of accuracy. Moreover, Naciri, Hauschild and Bisnath (2021) report significant improvements in PPP performance with the use of new Global Positioning System (GPS), Galileo, and BeiDou-2/3 signals, achieving horizontal and vertical Root Mean Square (RMS) of 2.3 and 2.6 cm, respectively, in static processing and 5.4 and 7.5 cm in kinematic processing after 1 hour of processing using real-time satellite correction products. The authors also found that mitigating known biases in GPS Block-IIF L5 can lead to average improvements of approximately 15% and 20% in horizontal and vertical RMS, respectively. These gains in PPP performances demonstrate the potential for continued advancement and improvement in PPP accuracy.

Given the importance of PPP and technological advances, it is crucial to analyze and understand the different configurations that allow the use of L5 and E5a carriers in data processing, evaluating their accuracy and trends. This study aims to contribute to the understanding of PPP applicability and limitations by analyzing processing configurations and assessing the kinematic PPP precision, trend, and accuracy. Nowadays, GNSS carrier frequencies are considered more modern and were developed to minimize noise, particularly in pseudorange measurements at the L1 band.

2 Methodology and Data

2.1 RTKLIB

The software RTKLIB performs the analysis of pseudorange and phase propagated through models integrated into its library, and being open source, there is the possibility of adding new algorithms through the C/C++ programming language. Regarding the modules contained in the computational resource, RTKLIB has RTKPOST (for post-processing), RTKPLOT (for a solution and data visualization), RTKNAVI (for retention, decoding, and conversion of GNSS data transmitted in real-time), and RTKCONV (for RINEX data format conversion). It is important to highlight that RTKLIB allows for the processing of multi-constellation GNSS and supports dual and triple-frequency observations.

The Receiver Independent Exchange Format (RINEX) format consists of a text file for observation data, navigation messages, and meteorological data for a specific date and receiving station, containing a header for general information and a data section. The data section includes code pseudorange (in meters), carrier phase, and observation time, recorded according to the receiver clock. The clock correction files contain solutions for GNSS time synchronization errors. Additionally, another file that can be used is the Ionosphere Map Exchange Format (IONEX), which stores maps of Vertical Total Electron Content (VTEC) and daily values of GNSS differential code polarization, derived from GNSS data.

The satellite orbit file is essential because its motion around the Earth has an associated force, which pushes it away from the Earth. As for the navigation RINEX file, the broadcasted ephemeris contains position, velocity, and clock information for all GNSS constellation satellites for each day. The antenna calibration files are in the Antenna Exchange Format (ANTEX), aiming for absolute corrections of the antenna phase center.

Regarding the UFPR station data processing, when requesting the program to process triple-frequency data with IONEX ionospheric correction type, the generated outputs had an RMS that exceeded the decimetric range. The RMS allows analyzing the accuracy between the GNSS tracking values and the considered true values. Finally, to solve the problem, the Slant Total Electron Content (STEC) estimation was used.

2.2 Selected Stations

The selected workstations were UFPR, located in Curitiba, Paraná, and the POVE station, located in Porto Velho, Rondônia, both belonging to Brazilian Network for Continuous Monitoring of GNSS (RBMC) (Figure 1).

RBMC is a network of GNSS stations established in Brazil to provide accurate and reliable positioning data. The network is managed by Brazilian Institute of Geography and Statistics (BIGS) and plays a crucial role in supporting various applications such as surveying, mapping, and geodetic studies.

Figure 1 Location of used RBMC stations in Brazil.

Given this, the tracking months chosen on the BIGS digital site were January 2022 for UFPR and July of the same year for POVE. Therefore, there are higher TEC values during months near the equinoxes and lower during winter months. In addition, ionospheric scintillation, which is a rapid variation in amplitude and phase of radio wave signals when these signals pass through ionospheric irregularities, is greater in regions near the magnetic equator, as stated by Pacini and Raulin (2006). Consequently, as it is the function of L5 and E5a observables to perform strongly in locations affected by multipath and ionospheric effects, it was expected that the addition of new carriers would improve the accuracy output quality of the post-processing of the selected stations.

2.3 GNSS Processing

The positioning mode employed in this study is PPP Kinematic, which utilizes different frequency combinations for the satellite signals. Two configurations were used: L1+L2/E5b and L1+L2/E5b+L5/E5a. The filter type selected for processing is Forward. Two elevation masks were tested: 15° and 10°, determining the minimum elevation angle for satellites to be included in the solution. Receiver dynamics were turned off, indicating that dynamic positioning was not utilized. Solid model earth tides correction was applied, and ionosphere correction was performed by estimating the Total Electron Content (TEC). The recording interval for the data was set to 1 second, ensuring regular sampling of the measurements. According to the sample Table 1, the following parameters are displayed.

Regarding the elevation mask of the adopted settings, satellites will be excluded if they are below a certain elevation angle or have a low Signal to Noise Ratio (SNR). However, in some specific cases of this study, the elevation mask was removed to evaluate potential benefits in terms of ellipsoidal height estimation. By allowing lower-elevation satellites to contribute to the positioning solution in these selected cases, it is possible to assess if there are improvements in determining the ellipsoidal height component of the position. This analysis helps to understand the impact of removing the elevation mask on the accuracy and reliability of the PPP results.

Additionally, the processing was conducted to compare the PPP performance with and without the inclusion of L5/E5a bands. These carrier frequencies are considered more modern and were developed to minimize noise, particularly in pseudorange measurements.

Table 1 General positioning settings.

Class	Attribute
Positioning Mode	PPP Kinematic
Frequencies	L1+L2/E5b and L1+L2/E5b+L5/E5a
Filter Type	Forward
Elevation Mask	15° and 10°
Receiver Dynamics	Off
Earth Tides Correction	Solid Model
Ionosphere Correction	Estimate TEC
Recording Interval	1 Second

3 Results

3.1 UFPR Station Data Processing

The result for the UFPR station, on the Day of Year (DoY) 004/2022, tracking from 10:00 to 10:45 AM, 1 second of recording interval, with GPS and Galileo constellations, is shown in Figure 2.

The results revealed in this study highlight the influence of including the L5/E5a observable on the positioning performance at the UFPR station. As shown in Figure 2, the bias and RMS of the East and North coordinates, in meters, were improved by the addition of the L5/E5a observable, while the degradation in the Vertical component was minimal. These findings emphasize the advantages of considering L5/E5a signals when performing GNSS positioning.

It is worth noting that the inclusion of the L5/E5a signal deteriorated the ellipsoidal height precision by ~2%, as shown in Table 2. The decrease in precision was approximately 0.009 m, which may have significant implications in applications that require height accuracy. Therefore, the benefits of including the L5/E5a signal and the potential degradation in height precision should be carefully evaluated according to the specific requirements of each application.

As satellite signals pass through the Earth's atmosphere, they are affected by various layers such as the ionosphere and troposphere, which can cause delays and errors in GNSS positioning (Fonseca Junior 2002). As a result, when a satellite is closer to the horizon, the portion of these layers that the signal needs to pass through increases, which can significantly degrade the accuracy and precision of the positioning results. To mitigate this effect, an elevation mask can be applied to exclude satellites that are too close to the horizon (Mendes Da Rocha et al. 2017).

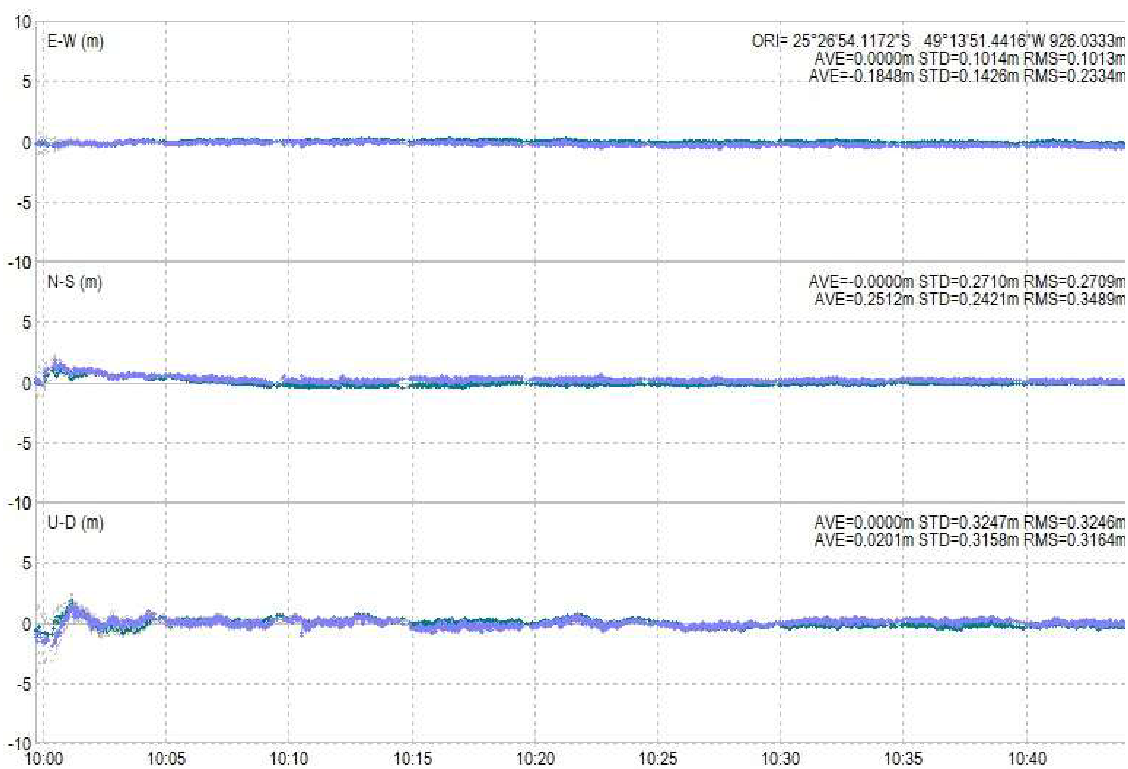

Figure 2 Comparison between dual and triple-frequency positioning with 15° elevation mask at UFPR station.

Table 2 Dual and triple-frequency accuracies with 15° elevation mask at UFPR station.

Coordinates	Double-Frequency RMS (m)	Triple-Frequency RMS (m)	RMS Gain (%)
E	0.233	0.101	~ +56.652
N	0.350	0.271	~ +22.571
UP	0.316	0.325	~ -2.848

However, to improve the quality of the altimetric positioning adjustment, making it more diverse in terms of observations, a 10° elevation mask was tested, which means that all satellites above this value were used in the solution. Moreover, all the other remaining parameters in Table 1 were kept unchanged. It is worth noting that while this approach may improve the vertical positioning component, it can potentially introduce errors in the horizontal positioning components due to the increased influence of the ionosphere and troposphere at lower elevation angles.

By analyzing the results presented in Figure 3 and Table 3, where the addition of the L5/E5a signal improved the East component by ~39%, the North component by ~34%, and the Up component by ~14%, it is evident that reducing the elevation mask to 10° in dual-frequency resulted in improvements in the East and North components, ~3% and ~21%, respectively, for dual-frequency, and ~33% in the North component for triple-frequency, when compared to the same test using the 15° elevation mask. However, reducing the elevation mask from 15° to 10° led to significant degradations in the Vertical component for both cases, with values exceeding ~100%, suggesting that reducing the elevation mask negatively impacts the adjustment of the input data.

About the required period to achieve a solution convergence time to a centimetric solution, it can be observed (Figures 2 and 3) that the period is nearly identical. To provide a more detailed analysis, Table 4 has been included to define the percentage gains relative to the comparison between the solutions obtained with the 15° and 10° masks, as presented in Tables 2 and 3, respectively. These percentage gains can be useful to assess the impact of a 10° mask. It is important to note that the convergence time can vary depending on several factors, such as the number and quality of the available satellites, the atmospheric conditions, and the positioning algorithm used. Table 4 shows the positioning gains and degradation found when reducing the elevation mask. East and North components exhibited significant gains when the elevation mask was reduced.

However, the evaluation of additional time frames to validate the previously made statements is found in Table 5, 45 minutes each.

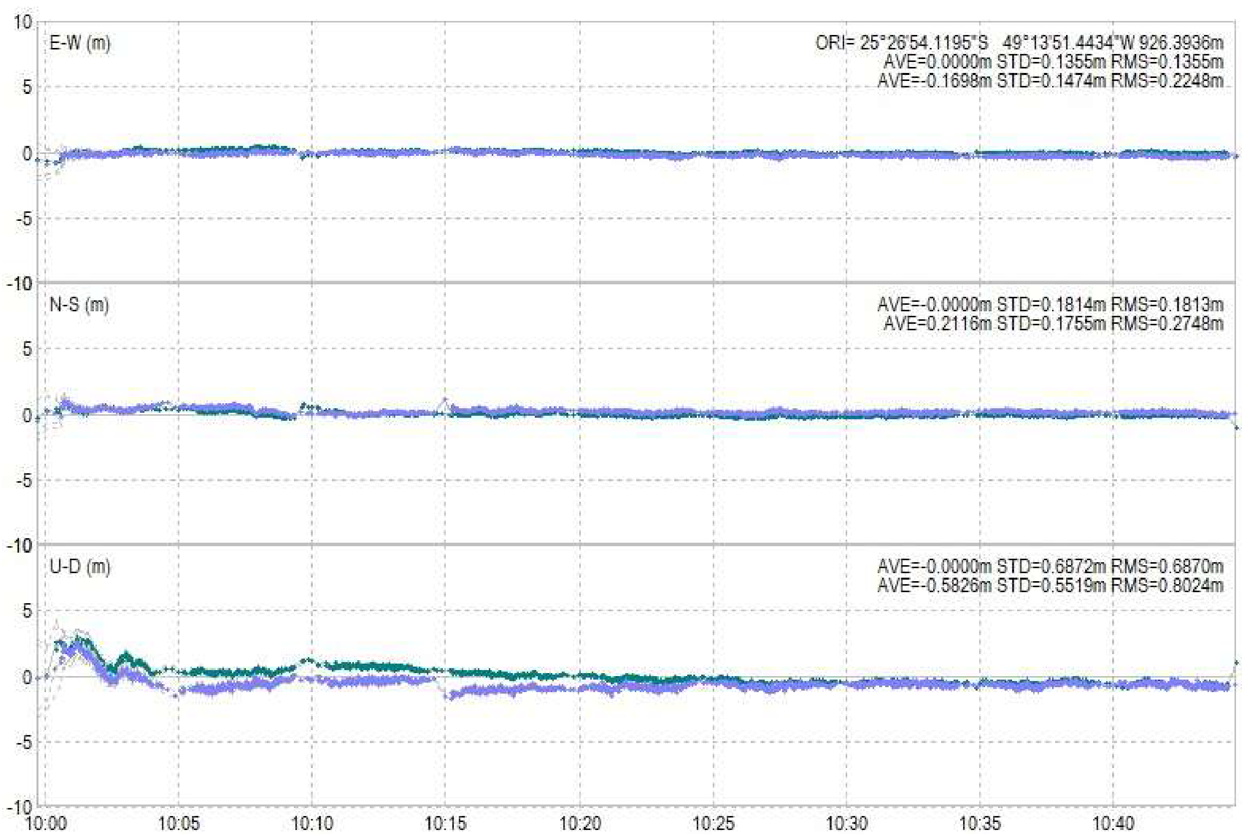

Figure 3 Comparison between dual and triple-frequency positioning with 10° elevation mask at UFPR station.

Table 3 Dual and triple-frequency accuracies with 10° elevation mask at UFPR station.

Coordinates	Double-Frequency RMS (m)	Triple-Frequency RMS (m)	RMS Gain (%)
E	0.225	0.136	~ +39.556
N	0.275	0.181	~ +34.182
UP	0.802	0.687	~ +14.339

Table 4 Percentual improvement gain with 10° elevation mask at UFPR station.

Coordinates	RMS Gain in Dual-Frequency (%)	RMS Gain in Triple-Frequency (%)
E	~ +3.433	~ -34.653
N	~ +21.429	~ +33.210
UP	~ -153.797	~ -111.385

Table 5 Tracking from 11:00 am to 6:45 pm at UFPR station with 15° elevation mask.

Coordinates	Double-Frequency RMS (m)	Triple-Frequency RMS (m)	RMS Gain (%)
Tracking Time: 11:00 to 11:45			
E	0.221	0.127	~ +74.016
N	0.278	0.173	~ +60.694
UP	0.821	0.576	~ +42.535
Tracking Time: 12:00 to 12:45			
E	0.208	0.118	~ +76.271
N	0.367	0.191	~ +92.147
UP	0.902	0.601	~ +50.083
Tracking Time: 13:00 to 13:45			
E	0.186	0.135	~ +37.778
N	0.267	0.189	~ +41.270
UP	0.817	0.674	~ +21.217
Tracking Time: 14:00 to 14:45			
E	0.213	0.180	~ +89.189
N	0.276	0.164	~ +68.293
UP	0.813	0.551	~ +47.550
Tracking Time: 15:00 to 15:45			
E	0.197	0.175	~ +12.571
N	0.223	0.173	~ +28.902
UP	1.008	0.392	~ +157.143
Tracking Time: 16:00 to 16:45			
E	0.287	0.208	~ +37.981
N	0.205	0.163	~ +25.767
UP	0.954	0.512	~ +86.328
Tracking Time: 17:00 to 17:45			
E	0.178	0.135	~ +31.852
N	0.213	0.178	~ +19.663
UP	0.997	0.644	~ +54.814
Tracking Time: 18:00 to 18:45			
E	0.178	0.113	~ +57.552
N	0.301	0.267	~ +12.734
UP	1.042	0.615	~ +69.431
Average Results			
E	0.209	0.149	~ +40.050
N	0.266	0.187	~ +42.189
UP	0.919	0.571	~ +61.093

3.2 POVE station data processing

The result for the POVE station, DoY 191/2022, tracking from 10:00 to 10:45 AM, with GPS and Galileo constellations, 1 second of recording interval, is given in Figure 4.

Figure 4 presents a comparison of the positioning results obtained with and without the use of the L5/E5a signal. The figure clearly shows that the addition of this observable has a positive impact on biases and RMS concerning the ground truth site coordinates, including the East and North components, as well as the ellipsoidal altitude, with gains exceeding ~50%. Moreover, the results presented in Table 6 corroborate this conclusion, demonstrating a significant improvement in the RMS values of the variables when the L5/E5a signal is included in the positioning solution. Therefore, the results obtained in this study suggest that the inclusion of the L5/E5a signal can be of utmost importance in improving the accuracy and reliability of GNSS positioning solutions, especially in challenging environments where the use of traditional signals may be limited by ionospheric and tropospheric effects.

Afterward, once again, the elevation mask was reduced, aiming to establish the reasoning discussed in section 3.1, for the UFPR station, as shown in Figure 5.

By analyzing the results generated in Figure 5, it can be concluded that the accuracy of the ellipsoidal altitude and the North coordinate obtained through dual-frequency data processing with the reduction of the elevation mask did not improve compared to the results presented in Figure 4. However, when considering only the triple-frequency data with the reduction of the elevation mask to 10° in a region with a more active ionosphere, significant improvements were observed in the North and Vertical components, with RMS gains exceeding ~60%. These findings suvggest that reducing the elevation mask in areas with a more variable ionosphere can be a viable approach when working with triple-frequency data.

Based on the results mentioned in the previous paragraph, it was possible to calculate the gains in terms of RMS, as shown in Table 7.

The convergence time of the solution is practically the same in Figures 4 and 5. Finally, Table 8 presents the gains, in percentage, regarding the comparison between the solutions obtained with elevation masks of 15° and 10°, as previously presented in Tables 6 and 7.

However, the evaluation of additional time frames to validate the previously made statements is found in Table 9, 45 minutes each.

The measured values over 45-minute time intervals at multiple times throughout the day reinforce the findings for the UFPR and POVE stations, as gains with the addition of the new observables are highlighted in the processing conducted using RTKLIB.

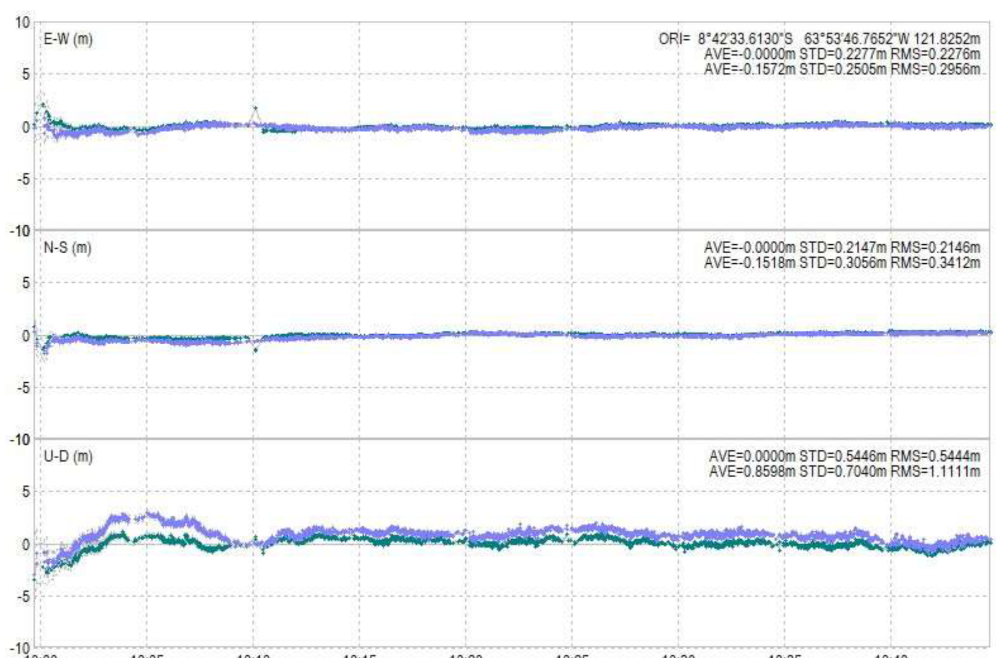

Figure 4 Comparison between dual and triple-frequency positioning with 15° elevation mask at POVE station.

Table 6 Dual and triple-frequency accuracies with 15° elevation mask at POVE station.

Coordinates	Double-Frequency RMS (m)	Triple-Frequency RMS (m)	RMS Gain (%)
E	0.296	0.228	~ +22.973
N	0.341	0.215	~ +36.950
UP	1.111	0.544	~ +51.035

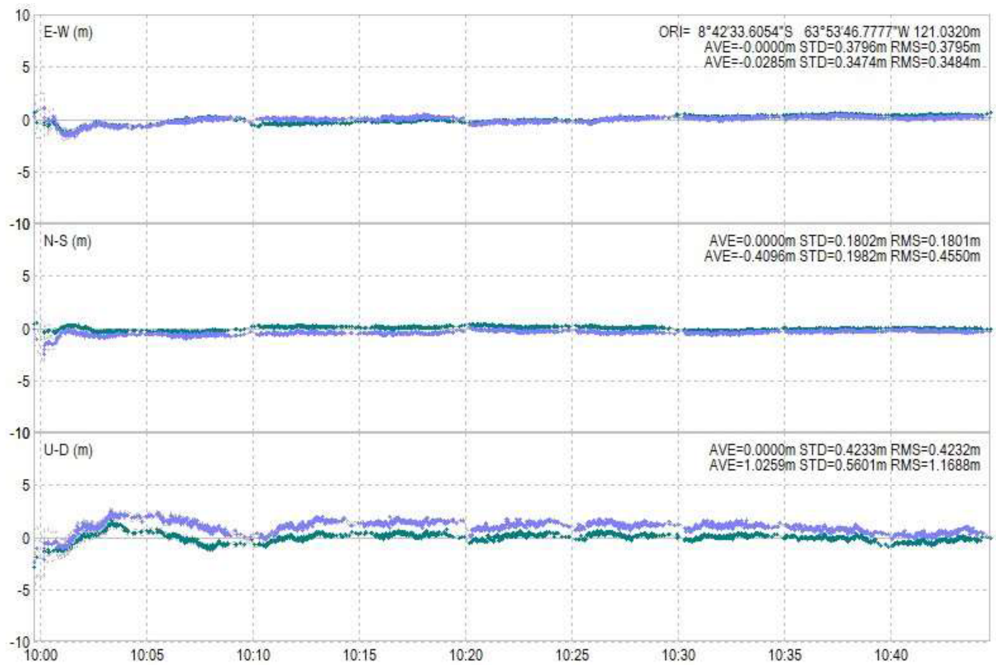

Figure 5 Comparison between dual and triple-frequency positioning with 10° elevation mask at POVE station.

Table 7 Precision of dual and triple-frequency with 10° elevation mask at POVE station.

Coordinates	Double-Frequency RMS (m)	Triple-Frequency RMS (m)	RMS Gain (%)
E	0.348	0.380	~ -9.195
N	0.455	0.180	~ +60.440
UP	1.169	0.424	~ +63.730

Table 8 Percentual improvement gain with 10° elevation mask at POVE station.

Coordinates	RMS Gain in Dual-Frequency (%)	RMS Gain in Triple-Frequency (%)
E	~ -17.568	~ -66.667
N	~ -33.431	~ +16.279
UP	~ -5.221	~ +22.059

Table 9 Tracking from 11:00 am to 6:45 pm at POVE station with 15° elevation mask.

Coordinates	Double-Frequency RMS (m)	Triple-Frequency RMS (m)	RMS Gain (%)
Tracking Time: 11:00 to 11:45			
E	0.367	0.339	~ +8.260
N	0.191	0.184	~ +3.384
UP	1.092	0.467	~ +133.833
Tracking Time: 12:00 to 12:45			
E	0.473	0.381	~ +24.147
N	0.310	0.284	~ +9.155
UP	0.981	0.587	~ +67.121
Tracking Time: 13:00 to 13:45			
E	0.273	0.221	~ +23.529
N	0.221	0.184	~ +20.109
UP	1.010	0.584	~ +72.945
Tracking Time: 14:00 to 14:45			
E	0.310	0.218	~ +42.202
N	0.290	0.131	~ +121.374
UP	0.847	0.452	~ +87.389
Tracking Time: 15:00 to 15:45			
E	0.264	0.198	~ +33.333
N	0.223	0.173	~ +28.902
UP	1.008	0.392	~ +157.143
Tracking Time: 16:00 to 16:45			
E	0.287	0.208	~ +7.981
N	0.205	0.163	~ +25.767
UP	0.954	0.512	~ +86.328
Tracking Time: 17:00 to 17:45			
E	0.266	0.297	~ -11.654
N	0.215	0.136	~ +58.088
UP	1.011	0.745	~ +78.307
Tracking Time: 18:00 to 18:45			
E	0.345	0.224	~ +54.018
N	0.426	0.365	~ +16.712
UP	0.998	0.593	~ +68.297
Average Results			
E	0.327	0.257	~ +27.300
N	0.260	0.203	~ +28.460
UP	0.988	0.542	~ +82.390

4 Conclusion

In the context of the conducted studies, reducing the elevation mask from 15° to 10° resulted in degradation in both analyzed frequencies. At the UFPR station, considering dual frequency, improvements were observed in the East and North components, approximately ~3% and ~21%, respectively. However, the Vertical component experienced a degradation of ~153%, indicating that the benefits of the reduction are not significant compared to the losses caused by the decrease in the elevation mask. For the triple frequency at the UFPR station, there was an RMS degradation in the East and Vertical components, approximately ~34% and ~111%, respectively, with gains of ~33% in the North component, which can be disregarded due to the losses caused by the reduction.

At the POVE station, located in a region with a more active ionosphere, the reduction of the elevation mask degraded all analyzed components in the dual frequency, with losses of ~17% in the East component, 33% in the North component, and ~5% in the Vertical component. In the case of triple frequency, the degradation in the East component was ~66%, with gains of ~16% and ~22% in the North and Vertical components, respectively.

Again, these gains are not relevant as the degradation in the East component was significant. Next, the benefits of including the L5/E5a signals were analyzed. In both stations, tracking was performed at different times of the day, with each session lasting 45 minutes, from 9:00 a.m. to 6:45 p.m. This allowed for estimating the average gains provided by the inclusion of these signals, considering a 15° elevation mask. In the East component, there was an average precision gain of ~33%, in the North component of ~35%, and in the Vertical component of ~71%.

Therefore, the inclusion of the L5/E5a observables provided overall benefits to the precision of the positioning solution, resulting in improvements in the results in all analyzed scenarios.

5 References

Alves, C.M.D., Monico, J.F.G. & Romão, V.M.C. 2011, 'Análise da Acurácia no PPP a Partir da Solução de Ambiguidades GPS em Curtos Períodos de Ocupação', *Revista Brasileira de Cartografia*, vol. 63, pp. 589-600, DOI:10.14393/rbcv63n0-43755.

Fonseca Júnior, E.S. 2002, 'O Sistema GPS como Ferramenta para Avaliação da Refração Ionosférica no Brasil', PhD Thesis, Universidade de São Paulo, São Paulo, DOI:10.11606/T.3.2002.tde-30102002-163432.

Grinter, T. & Roberts, C. 2011, 'Precise Point Positioning: Where are we now?', *IGNSS Symposium*, International Global Navigation Satellite Systems Society, Sydney, viewed 18 March 2024, <https://www.spatial.nsw.gov.au/__data/assets/pdf_file/0020/165701/2011_Grinter_and_Roberts_IGNSS2011_PPP_where_are_we_now.pdf>.

Grinter, T. & Roberts, C. 2013, 'Real time Precise Point Positioning: Are we there yet?', *IGNSS Symposium*, International Global Navigation Satellite Systems Society, Outrigger Gold Coast, viewed 23 April 2023, <https://www.spatial.nsw.gov.au/__data/assets/pdf_file/0005/184937/2013_Grinter_and_Roberts_IGNSS2013_real_time_PPP_are_we_there_yet.pdf>.

Huber, K., Heuberger, F., Abart, C., Karabatic, A., Weber, R. & Berglez, P. 2010, 'PPP: Precise Point Positioning - Constraints and Opportunities', *FIG Congress 2010*, Facing Challenges - Building the Capacity, Sydney, pp. 1-17, viewed 23 April 2023, <http://hdl.handle.net/20.500.12708/42639>.

Janssen, V. & McElroy, S. 2013, 'Virtual RINEX: Science or fiction?', *Position*, no. 67, pp. 38-41, viewed 23 April 2023, <https://hdl.handle.net/102.100.100/493561>.

Mendes Da Rocha, R.S., Jerez, G.O., Brassarote, G.O.N. & Monico, J.F.G. 2017, 'Avaliação do efeito da cintilação ionosférica e de diferentes intervalos de tempo de coleta de dados no Posicionamento por Ponto Preciso na sua forma on-line', *Revista Brasileira de Geomática*, vol. 5, no. 2, pp. 251-76, DOI:10.3895/rbgeo.v5n2.5429.

Naciri, N., Hauschild, A. & Bisnath, S. 2021, 'Exploring signals on L5/E5a/B2a for Dual-Frequency GNSS Precise Point Positioning', *Sensors*, vol. 21, no. 6, 2046, DOI:10.3390/s21062046.

Pacini, A.A. & Raulin, J. 2006, 'Solar X-ray flares and ionospheric sudden phase anomalies relationship: A solar cycle phase dependence', *Journal of Geophysical Research: Space Physics*, vol. 111, no. A9, A09301, DOI:10.1029/2006JA011613.

Rizos, C., Janssen, V., Roberts, C. & Grinter, T. 2012, 'Precise Point Positioning: Is the era of differential GNSS positioning drawing to an end?', *FIG Working Week 2012*, Rome, pp. 6-10, viewed 23 April 2023, <https://hdl.handle.net/102.100.100/520263>.

Zanetti, G.Z. 2018, 'Comparação dos Métodos de Posicionamento Relativo Estático e por Ponto Preciso (PPP) para Posicionamento com Bases Longas Voltado ao Monitoramento de Estruturas: Estudo de Caso para a Estação de Monitoramento Contínuo da UHE Mauá', Master Thesis, Universidade Federal do Paraná, Curitiba, viewed 23 April 2023, <https://hdl.handle.net/1884/62059>.

Zumberge, J.F., Heflin, M.B., Jefferson, D.C., Watkins, M.M. & Webb, F.H. 1997, 'Precise Point Positioning for the efficient and robust analysis of GPS data from large networks', *Journal of Geophysical Research: Solid Earth*, vol. 102, no. B3, pp. 5005-17, DOI:10.1029/96jb03860.

Author contributions
Osvaldo Tavares de Camargo Junior: conceptualization; formal analysis; methodology; validation; writing-original draft; writing – review and editing; visualization. Paulo Sergio de Oliveira Júnior: methodology; validation. Lucas dos Santos Bezerra: validation.

Conflict of interest
The authors declare no conflict of interest.

Data availability statement
All data included in this study are publicly available in the literature.

Funding information
Not applicable.

Como citar/How to cite:
Camargo Junior, O.T., Oliveira Júnior, P.S. & Bezerra, L.S. 2024, 'Perspectives for Improvements on Real-Time GNSS Positioning with the Use of New Observables' *Anuário do Instituto de Geociências,* 47:60380. https://doi.org/10.11137/1982-3908_2024_47_60380